Colin, T. M. Donahue, V. I. Moroz, Eds. (Univ. of Arizona Press, Tucson, 1983), pp. 484–564; D. Allen and J. W. Crawford, *Nature* **307**, 222 (1984); V. M. Linkin *et al.*, *Science* **231**, 1417 (1986); S. S. Limaye, *Icarus* **73**, 212 (1988); D. Crisp *et al.*, *Science* **246**, 506 (1989); W. B. Rossow, A. D. Del Genio, T. Eichler, *J. Atmos. Sci.* **47**, 2053 (1990).
4. M. J. S. Belton *et al.*, *J. Atmos. Sci.* **33**, 1383 (1976); M. J. S. Belton, G. R. Smith, G. Schubert, A. D. Del Genio, *ibid.*, p. 1394.
5. A. D. Del Genio and W. B. Rossow, *ibid.* **47**, 293 (1990).
6. K. Kawabata *et al.*, *J. Geophys. Res.* **85**, 8129 (1980).
7. R. G. Knollenberg and D. M. Hunten, *ibid.*, p. 8039.
8. B. O'Leary, *J. Atmos. Sci.* **32**, 1091 (1975).
9. D. Wallach and B. Hapke, *Icarus* **63**, 354 (1985).
10. G. Schubert, in *Venus*, D. M. Hunten, L. Colin, T. M. Donahue, V. I. Moroz, Eds. (Univ. of Arizona Press, Tucson, 1983), pp. 681–765.
11. P. J. Schinder, P. J. Gierasch, S. S. Leroy, M. D. Smith, *J. Atmos. Sci.* **47**, 2037 (1990).
12. M. J. S. Belton *et al.*, *Adv. Space Res.*, in press.
13. W. M. Irvine, *J. Atmos. Sci.* **25**, 610 (1968).
14. P. J. Gierasch, A. P. Ingersoll, R. T. Williams, *Icarus* **19**, 473 (1973); S. J. Ghan, *J. Atmos. Sci.* **46**, 2529 (1989).
15. G. Schubert, personal communication.
16. D. Crisp, *Icarus* **67**, 484 (1986); *ibid.* **77**, 391 (1989).
17. G. M. Yagi, J. J. Lorre, P. L. Jepsen, in *Proceedings of the Conference on Atmospheric Environment of Aerospace Systems and Applied Meterology* (American Meterological Society, Boston, 1978), pp. 110–117.
18. See, for example, C. C. Councelman, S. A. Gourevitch, R. W. King, G. B. Loriot, and E. S. Ginzberg [*J. Geophys. Res.* **85**, 8026 (1980)].
19. S. S. Limaye and V. E. Suomi, *J. Atmos. Sci.* **38**, 1220 (1981).
20. S. S. Limaye, C. J. Grund, S. P. Burre, *Icarus* **51**, 416 (1982); S. S. Limaye, C. Grassotti, M. J. Kuetemeyer, *ibid.* **73**, 191 (1988).
21. M. A. Williams, E. P. Krider, D. M. Hunten, *Rev. Geophys. Space Phys.* **21**, 892 (1983); Z. Levin, W. J. Borucki, O. B. Toon, *Icarus* **56**, 80 (1983).
22. W. J. Borucki *et al.*, *Geophys. Res. Lett.* **10**, 961 (1983).
23. J. B. Pollack *et al.*, *J. Geophys. Res.* **92**, 15037 (1987).
24. We gratefully acknowledge an internal review of the manuscript by G. Schubert and the assistance of H. Breneman, B. Carcich, C. Cunningham, E. DeJong, S. Howell, B. Paczkowski, T. Thompson, A. Toigo, and L. Wainio in the planning and execution of the SSI experiment and the subsequent reduction of the data.

21 June 1991; accepted 29 July 1991

Middle Infrared Thermal Maps of Venus at the Time of the Galileo Encounter

GLENN S. ORTON, JOHN CALDWELL, A. JAMES FRIEDSON, TERRY Z. MARTIN

Images of the disk of Venus, taken at wavelengths between 8 and 22 micrometers, were obtained a few days after the Galileo spacecraft's closest approach on 8 February 1990; these images show variations in the thickness of the main H_2SO_4 cloud deck and the overlying temperature structure. Several features are qualitatively similar to those of earlier observations, such as a hot region at the south pole, surrounded by a cold "collar," and brightening toward the lower latitudes, where low-contrast banding appears. The collar does have a northern counterpart that is warmer, however. Equatorial limb darkening is quantitatively similar to that of previous observations; fairly constant at wavelengths up to 20 micrometers, where limb darkening increases substantially. In contrast to what was found in previous observations, polar and equatorial limb darkening are nearly the same at most wavelengths. A longitudinal variation is observable that is consistent with a wavenumber-2 behavior and a brightness maximum near local midnight.

As PART OF A PROGRAM TO SUPPORT Galileo Venus science analysis and compare observations of the atmosphere of Venus with previous observations of the main H_2SO_4 cloud deck and overlying temperature structure, we imaged Venus on the mornings of 10, 11, and 12 February 1990 in the middle infrared. Poor weather prevented us from observing on 8 February, the day of the spacecraft's closest approach to Venus, or the following morning. We made the observations at the National Aeronautics and Space Administration (NASA) Infrared Telescope Facility at the summit of Mauna Kea at wavelengths of 8.57, 11.52, 13.00, 18.00, 20.24, and 21.88 µm. The wavelengths were chosen for comparison with earlier ground-based images (*1, 2*) and spatially resolved spacecraft data (*3–5*); the three longest wavelengths also overlap the spectral range of the Galileo Photopolarimeter-Radiometer (PPR) radiometric channels A, B, and C. The 60 pixel by 60 pixel images were produced by raster scanning in a regular grid pattern with 1-arc sec spacing in both directions; the entrance aperture was just under 2 arc sec in diameter. The disk of Venus, 23 to 25 days past inferior conjunction, subtended 49 arc sec, and the evening terminator was located about 42° east (Fig. 1) of the central meridian. We used the results of well-calibrated spacecraft experiments (*4, 5*) to normalize our absolute intensities.

G. S. Orton, A. J. Friedson, T. Z. Martin, Jet Propulsion Laboratory, California Institute of Technology, 4800 Oak Grove Drive, MS 169-237, Pasadena, CA 91109.
J. Caldwell, Physics Department, York University, 4700 Keele Street, North York, Ontario, Canada M3J 1P3.

The images from wavelengths of 8.57 and 11.52 µm (Fig. 1) show the greatest intensity contrast across the disk, a result of the strong dependence of their brightness on temperature. The east-west orientation of the scan rows is evident as narrow streaks, particularly near the limb of Venus, arising from short-term seeing and transparency variations. Evident in most of these images is a hot feature at the south pole. Hot features have been observed at the poles since the earliest thermal maps (*6*). This feature is consistent with Pioneer Venus Orbiter Infrared Radiometer (OIR) observations (*7*) of a bright, elongated feature at the north pole, rotating retrograde with a period of some 3 days. A much cooler "collar" surrounds the hot pole. Closer to the equator, the planet is brighter and contains lower contrast bands. None of these features is axisymmetric or stationary in earth- or solar-fixed coordinates.

The cold circumpolar collar and the brighter bands can also be seen in mosaics created from the images at each wavelength (Fig. 2). The direction of scans is evident as the nearly horizontal narrow bands sloping slightly upward toward higher longitudes. The best match of features contained in separate images implies an offset of roughly 90° in longitude per earth day, consistent with the 4-day retrograde period associated with ultraviolet features (*8*). The hot polar feature is confined to latitudes poleward of about 70°, and the collar is confined to latitudes between 50° and 70°, also consistent with the Pioneer Venus OIR results (*4, 7*). Except at 8.57 µm, the mosaics also show a cool region poleward of 45°N. The presence of a northern counterpart of the south pole collar is consistent with Galileo PPR maps and Near Infrared Mapping Spectrometer (NIMS) images of Venus from 5-µm thermal emission from the same cloud deck (*9*), but this collar is warmer than its southern counterpart. Images of the thermal emission of the night side of Venus at shorter wavelengths (*9, 10*) show a dark area near the pole that could correspond to the collar. Figure 2 shows a relatively bright streak between 30° and 50°S and a fainter streak between 20° and 40°S. There is no morphology in the Venus night side near-infrared data (*9, 10*) that immediately corresponds with these features. If the streaks are caused by a variation of cloud optical thickness, the cloud layer in question may be only one of several different components of a cloud system discernible at the shorter wavelengths.

The general morphology of brightness temperature features on Venus appears to be similar for all wavelengths greater than 8.57 µm, even at 13.00 and 18.00 µm, where the

Table 1. Mean brightness temperature changes.

λ (μm)	T_B (μ = 1.0) − T_B (μ = 0.5)* Equatorial	Polar (northern hemisphere)
8.57	9 ± 1	0 ± 1
11.52	12 ± 1	10 ± 2
13.00	9 ± 2	11 ± 1
18.00	12 ± 2	11 ± 1
20.24	17 ± 2	18 ± 1
21.88	19 ± 2	22 ± 1

*Emission angle cosine is denoted by μ.

radiation should be emerging from slightly higher levels in the atmosphere, owing to the increased CO_2 absorption. On the other hand, the morphology and limb darkening of the images at 8.57 μm (see Fig. 1 and Table 1) are sufficiently different to raise the possibility that there may be some additional opacity influencing this spectral region. This wavelength is close to a band of SO_2, but the 1983 Venera infrared spectra (*5*) do not show SO_2 absorption as a dominant influence on the 8.57-μm region, and the SO_2 atmospheric abundance was lower in 1990 than that in 1983 (*11*). More detailed modeling of the outgoing spectrum must be done in the context of latitudinally dependent temperature structure to resolve this issue.

We also compared the limb-darkening characteristics of the images with ground-based data in the 8- to 20-μm region (*2*) and with the Pioneer Venus OIR experiment (*4*). The mean brightness temperature (T_B) change between emission angle cosines of 1.0 and 0.5 are shown in Table 1 for all of the useful observations for two cases: (i) along the equator, similar to table 4 of Diner (*2*), and (ii) along the central meridian north of the sub-Earth point (more uniform in appearance than southward), similar to Diner's table 6 (*2*). For the equatorial data, the brightness temperature differences are quite uniform to 18.00 μm and are similar in value (9.7 to 11.2 K) to those of Diner. The values are much higher at 20.24 and 21.88 μm. Polar values are not measurably different, except at 8.57 μm and possibly 21.88 μm, in contrast with Diner's results (*2*) for data taken in 1975, which were characterized by consistently stronger limb darkening toward the poles than along the equator. This difference may indicate some variation over time of features on the disk, such as the circumpolar collar. The agreement between our observed 11.52-μm center-to-limb behavior and that of the Pioneer Venus OIR at 11.5 μm is also good. By implication, the vertical structure of clouds along the equator has not changed in any fundamental way since the 1975 ground-based or 1978–1979 Pioneer Venus OIR data. If we use a single deep cloud to model the atmospheric opacity at 11.52 and 20.24 μm in the context of a longitudinally averaged temperature structure derived from Pioneer Venus (*12*), the observed mean center-to-limb structure at the equator and middle latitudes is consistent with a particle scale height slightly smaller than the gas scale height. This result is consistent with the analysis of ground-based (*13*) and Pioneer Venus OIR (*14*) results. Furthermore, the ratio of the cloud opacity at 11.52 to 20.24 μm is about 1.4, which is consistent with the wavelength variation of the extinction of droplets of 75% by weight H_2SO_4 for a mean particle size of 1.5 μm (*15*).

Also present is a longitudinally dependent bifurcation of the center-to-limb structure. This dependence is also present at all wavelengths longer than 8.57 μm and can be seen quite clearly in the mosaics shown in Fig. 2 as a discontinuity between different maps, particularly at the longer wavelengths. This behavior is consistent with the presence of a wavenumber-2 longitudinal structure that produces greater thermal emission in the region near local midnight than near local dawn or dusk, as determined by ground-based (*12*) and spacecraft (*4*) results.

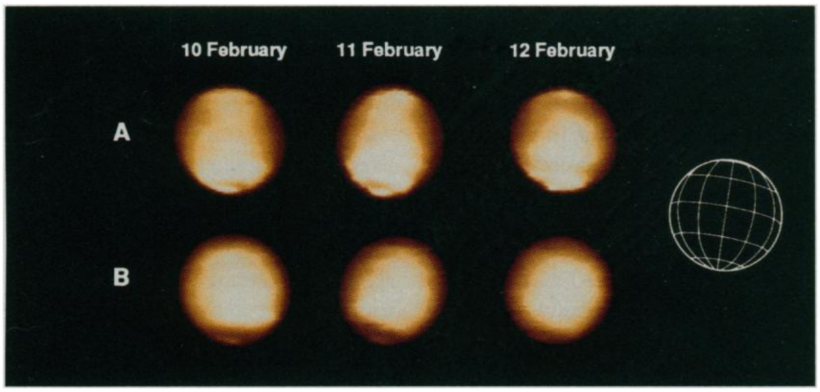

Fig. 1. Raster scan images of Venus at two of the six wavelengths used in this study; (**A**) 8.57 μm, (**B**) 11.52 μm. The oval shapes of some images result from deviations of telescope tracking from the true motion of Venus in the sky. The diagram of the planet shown to scale has latitudes and longitudes displayed at 30° intervals. A circle at the upper right illustrates the aperture size.

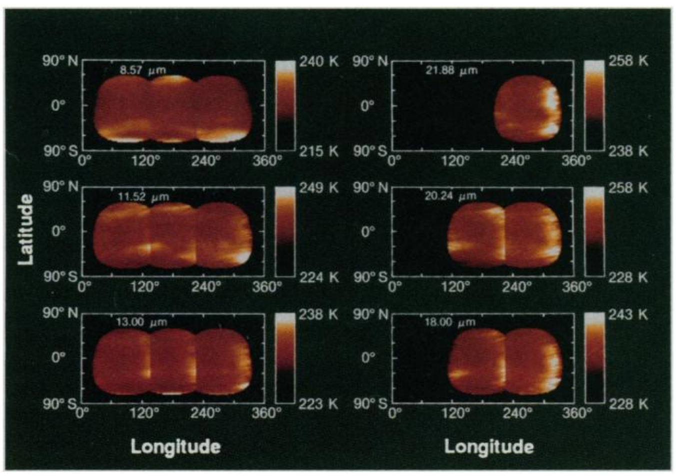

Fig. 2. Mosaics of the images at each wavelength. We created these by correcting for limb darkening using a two-term polynomial in emission angle cosine, converting to brightness temperature, and mapping onto a linear grid in latitude and longitude. We used only portions of images corresponding to 92% or less of the disk radius, avoiding sampling cold space near the limb and inaccuracies in fitting the planetary shape. The mosaics were created by joining the individual maps together to overlap features. The zero of longitude is arbitrary. The striking discontinuity at the longer wavelengths is a result of an asymmetric structure in each map, which is enhanced by a limb-darkening correction.

REFERENCES AND NOTES

1. Noteworthy ground-based middle infrared imaging studies of Venus are reported by D. J. Diner, J. A. Westphal, and F. P. Schloerb [*Icarus* **27**, 191 (1976)]; D. J. Diner and J. A. Westphal [*ibid.* **36**, 119 (1978)]; R. A. Brown and R. M. Goody [*ibid.* **35**, 189 (1978)]; J. Apt and R. Goody [*J. Geophys. Res.* **84**, 2529 (1979)]; J. Apt and R. Goody [*Science* **203**, 785 (1979)]; and J. Apt, R. A. Brown, and R. M. Goody [*J. Geophys. Res.* **85**, 7934 (1980)].
2. D. J. Diner, *J. Atmos. Sci.* **35**, 2356 (1978).
3. S. C. Chase, E. D. Miner, D. Morrison, G. Münch, G. Neugebauer, *Science* **183**, 1291 (1974).
4. F. W. Taylor *et al.*, *J. Geophys. Res.* **85**, 7963 (1980).
5. V. I. Moroz *et al.*, *Appl. Opt.* **25**, 1710 (1986).
6. B. C. Murray, R. L. Wildey, J. A. Westphal, *J. Geophys. Res.* **68**, 4813 (1963).
7. J. T. Schofield and D. J. Diner, *Nature* **305**, 116 (1983).
8. The earliest evidence for a 4-day retrograde period

of the winds at the cloudtop level, confirmed and refined by a variety of ground-based and spacecraft observations, was reported by C. Boyer and H. Camichel [*Ann. Astrophys.* **24**, 531 (1961)].
9. R. W. Carlson *et al.*, *Science* **253**, 1541 (1991).
10. D. Crisp *et al.*, *ibid.*, p. 1538.
11. L. W. Esposito *et al.*, *J. Geophys. Res.* **93**, 5267 (1988); C. Y. Na, L. W. Esposito, T. E. Skinner, *ibid.* **95**, 74 (1990); L. W. Esposito, personal communication.
12. G. M. Keating *et al.*, *Adv. Space Res.* **5**, 117 (1985).
13. D. J. Diner, J. Apt, L. S. Elson, *Icarus* **52**, 301 (1982), and references therein.
14. J. T. Schofield and F. W. Taylor, *Q. J. R. Meterol. Soc.* **109**, 57 (1983).
15. Assuming optical constants given by K. F. Palmer and D. Williams [*Appl. Opt.* **14**, 208 (1975)].
16. G.S.O., J. C., and T.Z.M. were visiting astronomers at the Infrared Telescope Facility (IRTF), which is operated by the University of Hawaii under contract to NASA. We thank the staff and management of the IRTF for their support, particularly site superintendent R. Koehler, and we thank IRTF Division Chief R. Joseph for his scheduling of these observations. NASA sponsored the work performed at the Jet Propulsion Laboratory (JPL), California Institute of Technology, and the National Research Council of Canada sponsored work performed at York University. G.S.O. and T.Z.M. particularly acknowledge support from the Galileo Project. We also appreciate the advice of D. J. Diner, J. V. Martonchik, and J. T. Schofield at various points in this work. N. Ha also provided essential data reduction support during his tenure at JPL as a Caltech Summer Undergraduate Research Fellow.

26 April 1991; accepted 18 July 1991

Ground-Based Near-Infrared Imaging Observations of Venus During the Galileo Encounter

D. Crisp, S. McMuldroch, S. K. Stephens, W. M. Sinton,*
B. Ragent, K.-W. Hodapp, R. G. Probst, L. R. Doyle,
D. A. Allen, J. Elias

Near-infrared images of Venus, obtained from a global network of ground-based observatories during January and February 1990, document the morphology and motions of the night-side near-infrared markings before, during, and after the Galileo Venus encounter. A dark cloud extended halfway around the planet at low latitudes ($<\pm 40°$) and persisted throughout the observing program. It had a rotation period of 5.5 ± 0.15 days. The remainder of this latitude band was characterized by small-scale (400 to 1000 kilometers) dark and bright markings with rotation periods of 7.4 ± 1 days. The different rotation periods for the large dark cloud and the smaller markings suggests that they are produced at different altitudes. Mid-latitudes ($\pm 40°$ to 60°) were usually occupied by bright east-west bands. The highest observable latitudes ($\pm 60°$ to 70°) were always dark and featureless, indicating greater cloud opacity. Maps of the water vapor distribution show no evidence for large horizontal gradients in the lower atmosphere of Venus.

Images of the night side of Venus taken at near-infrared (NIR) wavelengths (1 to 2.5 μm) reveal bright and dark markings that rotate from east to west with periods of about 6 days (*1, 2*). This infrared emission is produced by hot gases in the lower atmosphere (0 to 50 km). It is most intense at wavelengths near 1.74 and 2.3 μm, in the relatively transparent "spectral windows" between strongly absorbing CO_2 and H_2O bands in the Venus atmosphere. The planet-wide sulfuric acid (H_2SO_4) clouds provide the primary source of opacity in these windows (*2–6*). Kamp *et al.* (*4, 5*) found that 10 to 20% differences in the optical depths of the clouds could account for the contrast between bright and dark markings. They also derived water vapor mixing ratios near 40 parts per million by volume (ppmv) below the cloud base (47 km). This is 1/2.5 to 1/5 of that inferred from Pioneer Venus and Venera entry-probe measurements (*7–9*). More recent NIR imaging and spectroscopic observations (*6, 10–12*) support these conclusions and place new constraints on the composition and dynamics of the lower Venus atmosphere.

D. Crisp, MS 169-237, Jet Propulsion Laboratory, California Institute of Technology, Pasadena, CA 91109; visiting astronomer, Palomar Observatory, California Institute of Technology, Pasadena, CA 91125.
S. McMuldroch and S. K. Stephens, Division of Geological and Planetary Sciences, California Institute of Technology, Pasadena, CA 91125; visiting astronomers, Las Campanas Observatory, Casilla 601, La Serena, Chile.
W. M. Sinton, Institute for Astronomy, University of Hawaii, Honolulu, HI 96822.
B. Ragent, San Jose State University Foundation, San Jose, CA 95192; visiting astronomer, University of Hawaii 0.6-m and 2.2-m telescopes at Mauna Kea Observatory, Mauna Kea, Hawaii.
K.-W. Hodapp, Institute for Astronomy, University of Hawaii, Honolulu, HI 96822.
R. G. Probst, Kitt Peak National Observatory, Tucson, AZ 85719.
L. R. Doyle, National Aeronautics and Space Administration (NASA) Ames Research Center, Moffett Field, CA 94035; visiting astronomer, Kitt Peak National Observatory, Tucson, AZ 85719.
D. A. Allen, Anglo-Australian Observatory, Post Office Box 296, Epping, New South Wales, Australia.
J. Elias, Cerro Tololo Inter-American Observatory, Casilla 603, La Serena, Chile.

*Present address: Lowell Observatory, Flagstaff, AZ 86001.

The Galileo spacecraft's flyby of Venus on 10 February 1990 provided a novel opportunity to study the night-side NIR emission. The Galileo Near-Infrared Mapping Spectrometer (NIMS) acquired two high spatial resolution (25 to 50 km) maps of the Venus night side at 17 NIR wavelengths between 0.7 and 5.2 μm. This instrument also acquired complete NIR spectra of selected regions (*13*). To complement these spacecraft observations, a broad range of new NIR imaging and spectroscopic observations of Venus were acquired from a global network of ground-based observatories. The spectroscopic observations have been presented elsewhere (*6, 10–12, 14, 15*). The principal objective of the ground-based imaging program was to document the morphology and motions of the NIR markings before, during, and after the Galileo encounter. Thousands of NIR images were taken during the first week of January and during the first 2 weeks of February. These observing times were ideal for high-resolution imaging of the night side because Venus was near inferior conjunction (18 January 1990) with its night side facing Earth. Its angular size was about 50 arc sec, allowing about 50 resolution elements across the night side. Most images were taken in twilight or during the day because Venus was usually less than 30° from the sun. Images were collected almost continuously for 5- to 17-hour periods each observing day from sites that were widely separated in longitude (*16*). This high-resolution, long-duration time series allowed us to track a large number of distinct markings for periods ranging from 3 hours to 46 days (*17*).

The appearance of the Venus night side during January and February is shown in Figs. 1 and 2, respectively. These images were taken in the 2.3-μm spectral window where the NIR markings usually have the highest contrast. Low latitudes ($\pm 40°$) were characterized by a persistent large-scale (zonal wave number 1) pattern that moved from east to west (right to left in Figs. 2 and 3). The spatial extent of the bright and dark components of this pattern is more obvious in Fig. 3, A and B, where the imaging data from January and February, respectively, have been projected onto cylindrical latitude-longitude maps and combined to form global mosaics. A large, long-lived, dark patch that occupies this entire latitude range and covers about 180° of longitude was first seen on 1 to 2 January (Fig. 1, B and C), and again on 6 to 7 January (Fig. 1, F and G). Parts of it were also seen on 31 January, 5 February, and 10 to 12 February (Fig. 2, B and C and F through H). This dark patch, and a very similar feature seen in images taken in May and June 1988 (*2*), indicates the presence of increased H_2SO_4 cloud opacity (*4–6, 12, 15*).

Simulations of NIR spectra (*12, 15*) indicate that the darkest markings have 10 to 25%